The Journal of Antibiotics (2016) 69, 747–753

www.nature.com/ja

ORIGINAL ARTICLE

Studies on novel HIF activators, A-503451s. I. Producing organism, fermentation, isolation and structural elucidation

Yuki Hirota-Takahata[1], Hideki Kobayashi[2], Masaaki Kizuka[1], Takao Ohyama[3], Michiko Kitamura-Miyazaki[4], Yasuhiro Suzuki[5], Mie Fujiwara[1], Mutsuo Nakajima[1] and Osamu Ando[6]

In the course of our screening for activators of hypoxia-inducible factor (HIF), A-503451 A and virantmycin were isolated from the cultured broth of an actinomycete strain, *Streptomyces* sp. SANK 60101. From the same culture, the non-active homologs A-503451 B and D were also isolated. A-503451 A and virantmycin activated HIF-dependent reporter gene expression with EC_{50} values of 8 and 17 ng ml^{-1}, respectively. They are highly potent activators of HIF and thus may be therapeutically useful for erythropoiesis and neural cell protection.
The Journal of Antibiotics (2016) **69,** 747–753; doi:10.1038/ja.2016.17; published online 9 March 2016

INTRODUCTION

Hypoxia-inducible factor (HIF) is a heterodimeric transcription factor that senses decreased oxygen availability.[1] Under hypoxic conditions, activated HIF induces transcription of classical hypoxia-response genes and adapts cells to hypoxia. HIF induces erythropoietin and increases erythropoiesis.[2] It also induces vascular endothelial growth factor and promotes angiogenesis.[3] The activation of HIF promotes cell survival in hypoxic conditions such as ischemia and thereby protects the brain.[4] Therefore, the compounds that activate HIF under normoxic conditions may be useful as anti-anemic and anti-ischemic agents, and also for therapeutic angiogenesis. Recently, several HIF activators are now under clinical development of anti-anemia drug.[5] Discovering novel HIF-activating compounds would be useful not only for drug development but also for elucidating mechanisms underlying HIF regulation.

In the course of our screening for activators of HIF, potent activity was detected in the cultured broth of *Streptomyces* sp. SANK 60101 and two active compounds, A-503451 A and C (virantmycin[6]), and non-active homologs, A-503451 B and D, were isolated (Figure 1).

In this paper, we report on the producing organism, fermentation, isolation procedure, physico–chemical properties, structural elucidation and biological activities of A-503451s. Details of the biological activities of A-503451s were reported in a subsequent paper.[7]

RESULTS

Producing organism

As shown in Figure 2, the strain SANK 60101 formed *Rectinaculiaperti* spore chains, which are usually short, with 3–10 spores per chain, and may give rise to hooks, loops, incomplete spirals or spirals of only 1 or 2 turns. Most spores were elliptical and $0.4 \sim 0.6 \times 1.5 \sim 2.0$ μm in size with a smooth or rugose surface. The color of the substrate mycelium was pale yellow to grayish olive and that of the aerial spore mass was pale blue to bluish gray. Melanin pigment is neither produced on peptone–yeast extract agar nor on tyrosine agar. The temperature range for growth was from 14 to 45 °C. Growth occurs in media with 0% up to 3% sodium chloride. Starch, casein and gelatin were degraded. D-Glucose, L-arabinose, D-xylose, inositol, D-mannitol, D-fructose, L-rhamnose, sucrose and raffinose were all utilized for growth. Detection of LL-diaminopimelic acid in the whole-cell hydrolysates of the culture indicated that this strain had type I cell wall. The 16S ribosomal DNA sequence (1462 nucleotides) was determined and analyzed using EzTaxon-e database.[8] The result indicated that the gene sequences between SANK 60101 and *S. ipomoeae* NBRC 13050^T (AB184857) show 100% similarity. Based on the taxonomic properties described above, the strain was classified into *Streptomyces* sp.

Fermentation

One loopful growth of *Streptomyces* sp. SANK 60101 was transferred from an agar slant into a 2-l Erlenmeyer flask containing 450 ml of a primary seed medium composed of glucose 3%, pressed yeast 1%, soybean meal 3%, $CaCO_3$ 0.4%, $MgSO_4{\cdot}7H_2O$ 0.2% and Disfoam CB-442 (NOF Corp., Tokyo, Japan) 0.01%, pH 7.2. The flask was incubated at 28°C for 6 days on a rotary shaker at 210 r.p.m. The primary seed culture (450 ml) was transferred to a 30-l jar fermentor containing 15 l of a secondary seed medium that was identical to the

[1]Discovery Science and Technology Department, Daiichi Sankyo RD Novare Co., Ltd, Edogawa-ku, Tokyo, Japan; [2]Frontier Research Laboratories, Daiichi Sankyo Co. Ltd, Shinagawa-ku, Tokyo, Japan; [3]Venture Science Laboratories, Daiichi Sankyo Co. Ltd, Shinagawa-ku, Tokyo, Japan; [4]Biologics Pharmacology Research Laboratories, Daiichi Sankyo Co. Ltd, Shinagawa-ku, Tokyo, Japan; [5]Biologics Technology Research Laboratories, Daiichi Sankyo Co. Ltd, Oura-gun, Gunma, Japan and [6]Drug Metabolism and Pharmacokinetics Research Laboratories, Daiichi Sankyo Co., Ltd, Shinagawa-ku, Tokyo, Japan
Correspondence: Dr H Kobayashi, Frontier Research Laboratories, Daiichi Sankyo Co. Ltd, 1-2-58 Hiromachi, Shinagawa-ku, Tokyo 140-8710, Japan.
E-mail: kobayashi.hideki.gc@daiichisankyo.co.jp
Received 20 October 2015; revised 16 January 2016; accepted 25 January 2016; published online 9 March 2016

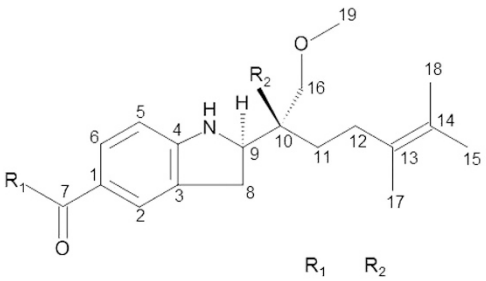

	R_1	R_2
A-503451 A (**1**)	OH	Cl
A-503451 B (**2**)	OH	OH
Benzastatin E	NH_2	OH

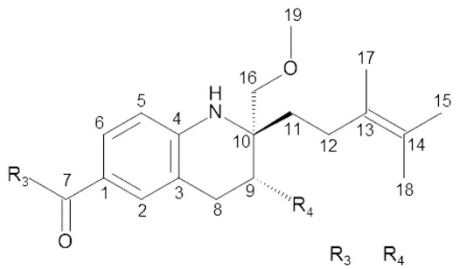

	R_3	R_4
Virantmycin (A-503451C, **3**)	OH	Cl
A-503451 D (**4**)	OH	OH
A-503451 D mesylate (**5**)	OH	OMs
A-503451 D acetylate (**6**)	OH	OAc
Benzastatin C	NH_2	Cl
Benzastatin D	NH_2	OH

Figure 1 Structures of A-503451s.

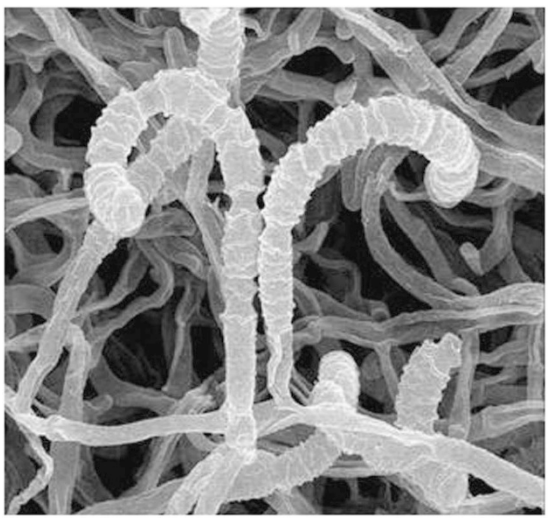

Figure 2 Scanned electron micrograph of strain. SANK 60101 on potato extract–carrot extract agar at 28 °C for 14 days.

primary seed medium. The cultivation was conducted for 24 h at 28°C with agitation (100–280 r.p.m.) and aeration (15 l per min). Then, a 9-l portion of the culture was transferred to a 600-l tank fermentor containing 300 l of a production medium, which was composed of sucrose 5%, pressed yeast 1%, soybean meal 3%, $CaCO_3$ 0.4%, $MgSO_4{\cdot}7H_2O$ 0.2% and Disfoam CB-442 0.01%, and was adjusted to pH 7.2 before sterilization. The fermentation was carried out for 7 days at 26°C with agitation (83–110 r.p.m.) and aeration (300 l per min).

Isolation of A-503451 A (1), B (2), C (3) and D (4)

An equal amount of acetone was added to the cultured broth (310 l). The extract was filtered using a filter press with the assistance of Celite 545 (Thermo Fisher Scientific Chemicals Inc., Waltham, MA, USA). The pH of the filtrate (570 l) was adjusted to 2.9 with 6 N HCl, and A-503451s were extracted with ethyl acetate (300 l). The organic layer was concentrated to dryness to give an oily substance (282.4 g). The substance was subjected to an ODS open column (Cosmosil 140C18-OPN, Nacalai Tesque, Inc., Kyoto, Japan, 14 liters). The chromatography was performed by stepwise elution using 40, 50 and 60% aq. MeCN.

The 60% aq. MeCN fraction containing **1** and **3** was concentrated to dryness, and then **1** and **3** were purified by preparative HPLC using an ODS column (YMC Pack R-3105-20AM, 100 i.d. × 500 mm, YMC Co., Ltd, Kyoto, Japan). The chromatography was performed with MeCN-0.5% triethylamine-phosphate (TEAP) buffer at pH 5.0 (3:2) at a flow rate of 250 ml per min. Active fractions containing **1** and **3** were collected separately followed by concentration and extraction with ethyl acetate. Each organic layer was concentrated to dryness to give **1** (960 mg) and **3** (4.88 g).

The 50% aq. MeCN fraction containing **2** and **4** was concentrated to dryness, and the following preparative HPLC using the same ODS column described above with MeCN-0.5% TEAP buffer pH 5.0 (9:11) at a flow rate of 240 ml per min gave **2** (1.55 g) and **4** (4.86 g).

Physico–chemical properties of 1–4

The physico–chemical properties are summarized in Table 1. According to the UV spectral data, the ^1H and ^{13}C NMR spectra in $CDCl_3$ (Table 2) and $[\alpha]^{25}_D$ in $CHCl_3$, **3** was identified as the known antibiotic, virantmycin.[6,9]

Structural elucidation of 1

The structural elucidation was mainly focused on **1**. The molecular formulae of **1** was determined to be $C_{19}H_{26}ClNO_3$ by positive ion high-resolution TOFMS (ESI). The ^1H and ^{13}C NMR spectral data of **1** obtained in DMSO-d_6 are summarized in Table 2. In the ^1H NMR spectrum of **1**, signals from three methyl groups (δ 1.60, 1.61 and 1.62), one methoxyl group (δ 3.34) and the aromatic system (δ 6.46–7.56) were observed. Observed proton signals, except for two deuterium exchangeable protons (δ 6.73 and 11.95), were attributed to each carbon by HSQC spectrum. In the ^{13}C NMR spectrum, 19 carbon signals were observed and classified into 4× methyl, 4× methylene, 4× methine and 7 quaternary carbons through analysis of the ^1H, ^{13}C NMR and HSQC spectra. The existence of nine sp^2 carbons strongly suggested the presence of one aromatic system, one olefinic linkage and one carbonyl group. Together with these data, two deuterium exchangeable protons were suggestive of the presence of a secondary amine and a carboxyl group.

The partial structure except for the attached site of the chlorine was elucidated by several NMR techniques such as DQFCOSY, HSQC and HMBC. The DQFCOSY spectrum clarified three spin systems from H-5 to H-6, H-8 to NH-9 and H-11 to H-12. In the HMBC spectrum, observed C–H long-range correlations clearly revealed the key structure as shown in Figure 3. In particular, the correlations between

Table 1 Physico–chemical properties of A-503451s

	*A-503451 A (**1**)*	*A-503451 B (**2**)*	*A-503451 C (**3**)*	*A-503451 D (**4**)*
Appearance	White powder	White powder	White powder	White powder
Molecular formula	$C_{19}H_{26}ClNO_3$	$C_{19}H_{27}NO_4$	$C_{19}H_{26}ClNO_3$	$C_{19}H_{27}NO_4$
HR-TOFMS (*m/z*)				
Found	352.1664 $(M+H)^+$	334.2003 $(M+H)^+$	352.1685 $(M+H)^+$	334.2003 $(M+H)^+$
Calcd.	352.1679 (for $C_{19}H_{27}ClNO_3$)	334.2018 (for $C_{19}H_{28}NO_4$)	352.1679 (for $C_{19}H_{27}ClNO_3$)	334.2018 (for $C_{19}H_{28}NO_4$)
$[\alpha]^{25}_D$	+71° (*c* 0.5, MeOH)	+30° (*c* 0.5, MeOH)	−14° (*c* 0.51, $CHCl_3$)	−14° (*c* 0.51, MeOH)
UV$\lambda_{max\ (nm)}$ (ε) (MeOH)	205 (33 000), 227 (12 000), 308 (24 000)	204 (30 000), 226 (11 000), 307 (19 000)	205 (36 000), 227 (11 000), 307 (27 000)	205 (31 000), 229 (10 000), 309 (24 000)
IR ν_{max} (cm^{-1}) (KBr pellet)	3402, 2983, 2924, 1672, 1610, 1503, 1455, 1431, 1271, 1120, 774	3411, 3353, 2983, 2924, 1671, 1610, 1503, 1455, 1433, 1270, 1113, 774	3411, 2983, 2924, 1673, 1609, 1517, 1432, 1289, 1254, 1131, 1110, 774	3404, 2981, 2926, 1672, 1607, 1517, 1433, 1288, 1254, 1132, 1108, 774
HPLC[a] RT (min)	9.9	4.3	8.9	3.7

Abbreviation: RT, retention time.
[a]YMC AM-312-3 (6 i.d. × 150 mm), MeCN-0.3% triethylamine-phosphate buffer at pH 5.0 (3:2), 1.5 ml per min

NH-9 and C-8, H-8 and C-3, and H-8 and C-4 indicated that **1** has an indoline skeleton and not a tetrahydroquinoline skeleton similar to virantmycin. Although there was no direct evidence of the chlorine binding position, the only appropriate position was axiomatically determined to be the sp^3-quaternal carbon at C-10. The chemical shift value of C-10 (δ 78.5) well explained the structure.

In order to determine the relative stereochemistry, a J-HMBC spectrum [10,11] was attempted. However, the spectrum of **1** showed the medium value of $^3J_{C\text{-}16,H\text{-}9}$ (3.51 Hz), and the other consequential correlation peak between C-11 and H-9 was too weak to clarify their coupling constant. Therefore, the relative stereochemistry was determined by ROESY spectrum.[12] In the ROESY spectrum, key correlations between H-9 and H-$16_{a,b}$, and between H-$8_{a,b}$ and H-$11_{a,b}$ were observed. When H-9 is assumed to be a pseudo-axial α-oriented proton, that is, the position 9 is *R**, observed these ROEs surely indicate that the position 10 is *S** as shown in Figure 3. Furthermore, observed ROE between H-12 and H-$16_{a,b}$ also supported the result. Thus, the relative configuration of **1** was elucidated as (9*R**, 10*S**).

Structural elucidations of 2 and 4

As shown in Table 1, the molecular formulae of **2** and **4** had one less chlorine atom, one more hydrogen atom and one more oxygen atom than those of **1** and **3**, respectively.

Together with the IR and UV spectral data, the chemical shifts of ^1H and ^{13}C NMR signals of **2** in DMSO-d_6 (Table 2) were closely similar to those of **1**, except for the presence of three deuterium exchangeable protons. These data indicated that a chlorine atom at C-10 in **1** was replaced by a hydroxyl group in **2**. Further comparison study of the 2D-NMR spectra, including the HMBC spectrum, with those of **1** revealed the structure of **2** as shown in Figure 1.

The relative stereochemistry of **2** was carried out in the same way as **1**. As the signals of H-16_a and H-16_b in DMSO-d_6 overlapped (δ 3.30, 2H, m), the NMR analyses were carried out in $CDCl_3$ and the signals were observed separately (H_a: δ 3.44, 1H, d, J = 9.2 Hz and H_b: δ 3.53, 1H, d, J = 9.2 Hz). In the ROESY spectrum, the observed key correlations between H-$8_{a,b}$ and H-$11_{a,b}$, H-9 and H-16_b, and H-12 and H-16_a revealed the relative configurations at C-9 and C-10 as *R** and *S**, respectively, which were the same as **1** as shown in Figure 4. The J-HMBC spectrum of **2** showed the small values of $^3J_{C\text{-}11,H\text{-}9}$ (2.38 Hz) and $^3J_{C\text{-}16,H\text{-}9}$ (2.38 Hz). It indicated that the orientations between H-9 and C-11, and between H-9 and C-16 are in gauche, which means that H-9 and a hydroxyl group at C-10 are in anti. These results well explained the relative configurations of C-9 and C-10 derived from the ROESY data.

In the case of **4**, the IR and UV spectral data, and the ^1H and ^{13}C NMR spectra in $CDCl_3$ (Table 2) were closely similar to those of **3**. As described above, **4** was the novel 9-dechloro-9-hydroxyl homolog of **3**. The stereochemistry of **4** was determined by J-HMBC and NOESY. In the J-HMBC spectrum, **4** showed the large value of $^2J_{C\text{-}9,H\text{-}8a}$ (6.47 Hz) and the small value of $^2J_{C\text{-}9,H\text{-}8b}$ (3.04 Hz), which indicated that the orientation of a hydroxyl group at C-9 and H-8_a is in gauche, and the hydroxyl group and H-8_b is in anti. In the NOESY spectrum, the observed key correlation between H-8_b and H-$11_{a,b}$ finally revealed the relative configurations at C-9 and C-10 as *R** and *R**, respectively, as shown in Figure 4. On the other hand, an NOE correlation between H-8_a and H-16_b was also observed. The data revealed that **4** was also able to form 1,3-diaxial conformation between H-8_a and C-16, which is the same stereochemical ambiguity as virantmycin[13] and benzastatin D.[14,15]

Biological activities

As shown in Table 3, **1** and **3** activated HIF with EC_{50} values of 8 and 17 ng ml^{-1}, respectively. In contrast, **2** and **4** did not activate HIF even at high concentrations (EC_{50} > 5 μg ml^{-1}).

Two active compounds, **1** and **3**, have a chlorine atom in the molecule, whereas non-active homologs, **2** and **4**, have a hydroxyl group instead. In order to investigate the role of the chlorine atom in their activities, we focused on the leaving group and synthesized two derivatives modified at the C-9 position of **4**. The 9-mesyl (Ms) derivative (**5**) showed potent activity equal to **1**, but the 9-acetyl derivative (**6**) did not show the same activity. Details of the biological activity of A-503451 A were reported in a subsequent paper.

DISCUSSION

In the course of our screening for the activators of HIF, two active compounds A-503451 A (**1**) and C (**3**), and non-active homologs, B (**2**) and D (**4**), were isolated from the cultured broth of *Streptomyces* sp. SANK 60101. The structures of **1**, **2** and **4** were elucidated from their physico–chemical and spectral data, and they were shown to be new compounds.

The structural difference among them was that a chlorine atom at C-10 in **1** (or C-9 in **3**) was replaced by a hydroxyl group in **2** (or **4**).

Table 2 ^{1}H and ^{13}C NMR signal assignments of A-503451s

	*A-503451 A (**1**)*		*A-503451 B (**2**)*	
Position	δ_C	δ_H	δ_C	δ_H
NH		6.73 (1H, d, 2.1 Hz)		6.34 (1H, d, 1.4 Hz)
1	118.1 (s)		117.5 (s)	
2	125.2 (d)	7.51 (1H, br. s)	125.2 (d)	7.48 (1H, br. s)
3	127.2 (s)		128.0 (s)	
4	155.6 (s)		156.3 (s)	
5	106.0 (d)	6.46 (1H, d, 8.0 Hz)	105.9 (d)	6.43 (1H, d, 8.3 Hz)
6	130.3 (d)	7.56 (1H, dd, 1.7, 8.0 Hz)	130.2 (d)	7.53 (1H, dd, 1.6, 8.3 Hz)
7	167.4 (s)		167.5 (s)	
8	30.4 (t)	H_a 3.01 (1H, dd, 7.7, 16.7 Hz), H_b 3.11 (1H, dd, 10.3, 16.7 Hz)	28.8 (t)	H_a 2.89 (1H, dd, 9.7, 16.4 Hz), H_b 2.97 (1H, dd, 9.0, 16.4 Hz)
9	63.4 (d)	4.28 (1H, ddd, 2.6, 8.1, 10.3 Hz)	64.2 (d)	3.97 (1H, dd, 1.9, 9.5 Hz)
10	78.5 (s)		73.2 (s)	
11	33.3 (t)	H_a 1.68 (1H, ddd, 5.1, 12.0, 14.5 Hz) H_b 1.79 (1H, ddd, 5.1, 11.5, 14.1 Hz)	31.8 (t)	1.37 (2H, m)
12	28.4 (t)	2.12 (2H, m)	27.6 (t)	H_a 1.97 (1H, dt, 5.6, 11.8 Hz) H_b 2.06 (1H, dt, 4.9, 12.2 Hz)
13	126.5[a] (s)		127.7 (s)	
14	124.0[a] (s)		122.8 (s)	
15	19.6[b] (q)	1.62 (3H, s)	19.6[a] (q)	1.60 (3H, s)
16	73.9 (t)	H_a 3.58 (1H, d, 10.3 Hz), H_b 3.62 (1H, d, 10.3 Hz)	75.0 (t)	3.30 (2H, m)
17	18.2 (q)	1.60 (3H, s)	18.2 (q)	1.57 (3H, s)
18	20.3[b] (q)	1.61 (3H, s)	20.3[a] (q)	1.57 (3H, s)
19	58.6 (q)	3.34 (3H, s)	58.6 (q)	3.29 (3H, s)
COOH		11.95 (1H, br. s)		11.87 (1H, br. s)
10-OH				4.26 (1H, br. s)

	*A-503451 C (**3**)*		*A-503451 D (**4**)*	
Position	δ_C	δ_H	δ_C	δ_H
1	117.5 (s)		117.8 (s)	
2	132.5 (d)	7.77 (1H, d, 2.0 Hz)	133.2 (d)	7.78 (1H, d, 2.1 Hz)
3	116.1 (s)		117.0 (s)	
4	147.2 (s)		147.4 (s)	
5	113.6 (d)	6.53 (1H, d, 8.6 Hz)	113.4 (d)	6.50 (1H, d, 8.6 Hz)
6	130.4 (d)	7.76 (1H, s)	130.2 (d)	7.75 (1H, dd, 2.1, 8.1 Hz)
7	171.1 (s)		171.7 (s)	
8	33.5 (t)	H_a 3.11 (1H, dd, 6.0, 17.0 Hz), H_b 3.37 (1H, dd, 5.0, 17.0 Hz)	32.7 (t)	H_a 2.86 (1H, dd, 6.0, 17.1 Hz) H_b 3.11 (1H, dd, 4.3, 17.1 Hz)
9	56.2 (d)	4.36 (1H, dd, 4.5, 6.0 Hz)	67.4 (d)	3.99 (1H, dd, 4.7, 6.0 Hz)
10	58.1 (s)		57.6 (s)	
11	33.6 (t)	H_a 1.61 (1H, ddd, 4.5, 12.1, 14.1 Hz) H_b 1.81 (1H, ddd, 5.0, 12.1, 14.1 Hz)	33.3 (t)	H_a 1.54 (1H, ddd, 5.1, 12.0, 14.1 Hz) H_b 1.82 (1H, ddd, 5.3, 11.8, 14.1 Hz)
12	27.8 (t)	H_a 2.01 (1H, dt, 4.0, 12.1 Hz) H_b 2.09 (1H, dt, 5.0, 12.1 Hz)	27.7 (t)	2.07 (2H, m)
13	126.5 (s)		126.8 (s)	
14	124.8 (s)		124.6 (s)	
15	19.9[a] (q)	1.61 (3H, s)	20.0[a] (q)	1.63 (3H, s)
16	74.0 (t)	H_a 3.55 (1H, d, 9.0 Hz) H_b 3.58 (1H, d, 9.0 Hz)	75.0 (t)	H_a 3.49 (1H, d, 9.4 Hz) H_b 3.67 (1H, d, 9.4 Hz)
17	18.5 (q)	1.63 (3H, s)	18.4 (q)	1.61 (3H, s)
18	20.6[a] (q)	1.61 (3H, s)	20.6[a] (q)	1.61 (3H, s)
19	59.4 (q)	3.39 (3H, s)	59.5 (q)	3.40 (3H, s)

Signal assignments of A-503451 A (**1**) and A-503451 B (**2**) are measured in DMSO-d_6, and signal assignments of A-503451 C (**3**) and A-503451 D (**4**) are measured in $CDCl_3$. Superscript letters 'a' and 'b' denote interchangeable.

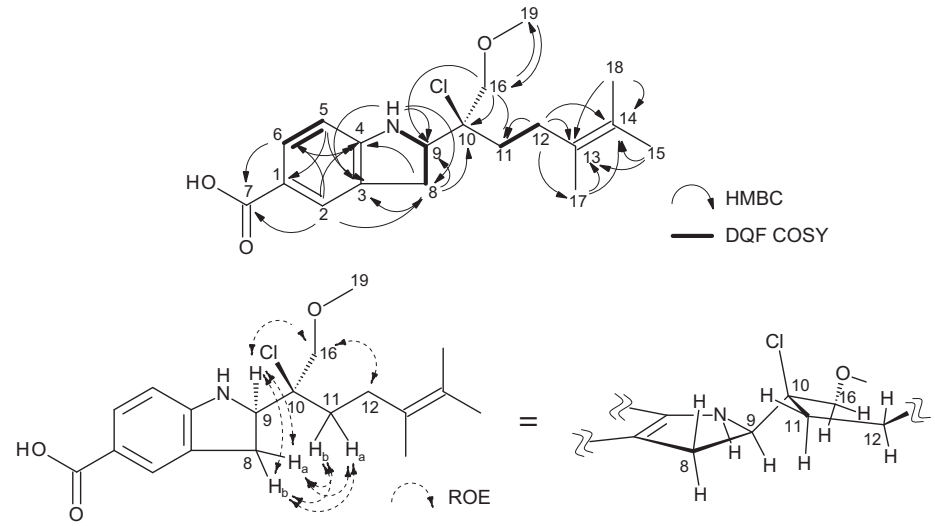

Figure 3 NMR data of A-503451 A (**1**).

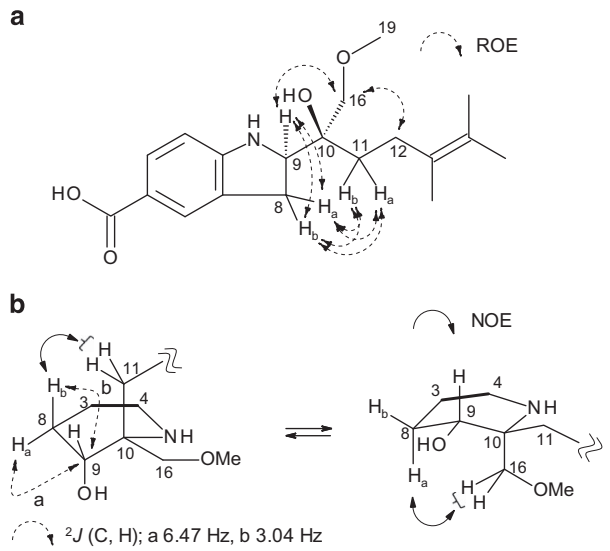

Figure 4 Stereochemistries of A-503451 B (**2**) and D (**4**). (**a**) ROE data of A-503451 B (**2**). (**b**) NOE data of A-503451 D (**4**).

However, the relative stereochemistries of **1** and **2** (or **3** and **4**) was the same. It seems to indicate that **1** and **2** (or **3** and **4**) were not formed by the substitution reaction at C-10 (or C-9), but formed by an attack of the nucleophile to the same side of a common intermediate.

Among known antibiotics, the structures of **1**, **2** and **4** resemble those of virantmycin and benzastatin C, D and E, including their relative stereochemistry. Benzastatins were reported to have free-radical-scavenging activity. Although it remains a necessity to examine the radical scavenging activities of A-503451s, we concluded that the radical scavenging activity of these compounds is not the cause of HIF activation for the following reasons. Benzastatin C has a chlorine atom and D has a hydroxyl group, and their free-radical-scavenging activities are reported to be mostly equal.[12,14] Therefore, the chlorine at C-9 position of benzastatin C is not essential to its radical scavenging activity. On the other hand, for A-503451s, the existence

Table 3 Induction activities of A-503451s on pGVB2-EPO-Luc reporter assay.

Compounds	*EC_{50} (ng ml^{-1})*
1	8
2	>5000
3	17
4	>5000
5	10
6	>5000

of the chlorine atom at C-9 position of **3** or C-10 position of **1** is essential to the activation of HIF.

We discovered some clues to the mechanism of HIF activation in the structures of A-503451s. One comes from the identification of two types of skeletons as HIF activators: **1** has an indoline skeleton and **3** has a tetrahydroquinoline skeleton. Although they have different skeletons, both compounds have a chlorine atom at β-position of the nitrogen and, in fact, both are β-halogenoamine. Another clue is the difference in the activities between **3** and **4** (or between **1** and **2**). In order to investigate the critical property of the group at C-9 position required for the activity, we synthesized two derivatives modified at the C-9 position of **4**. As a result, the chlorine was exchangeable for a mesyl group, but not for an acetyl group.

Taken together, the good leaving groups (for example, chlorine or mesyl) at β-position of the nitrogen were shown to be necessary for A-503451s as HIF activators. This seems to indicate that the substitution reaction (or elimination), which was concerned with the leaving group, occurs in the process of HIF activation. A-503451s themselves may react with the target protein through the substitution reaction, or an active intermediate may be formed through the substitution reaction. Although there is no straightforward data to support these hypotheses, it is reasonable to propose that A-503451s, or an active intermediate, modify the activity of the target through the formation of a covalent bond to the protein. As the details of the mechanism of HIF activation remains to be identified, the series of compounds reported in this paper will be good molecular probes to investigate the hypoxic response.

EXPERIMENTAL PROCEDURE

General experimental procedures

IR spectra were obtained on a JASCO FT/IR-610 spectrometer (JASCO Corp., Tokyo, Japan). UV spectra were recorded on an UV-265FW spectrometer (Shimadzu Corp., Kyoto, Japan). NMR spectra were recorded on an AVC500 spectrometer (Bruker Corp., Billerica, MA, USA) equipped with a cryogenic probe. High-resolution mass spectra were recorded on a Micromass LCT spectrometer (Waters Corp., Milford, MA, USA). Atomospheric pressure chemical ionization (APCI) mass spectra and electrospray ionization (ESI) mass spectra were recorded on an Agilent 1100 series LC/MSD (Agilent Technologies, Santa Clara, CA, USA).

Taxonomic studies

The producing organism, strain SANK 60101, was isolated from a soil sample collected in Ibaraki Prefecture, Japan in 1994. Methods described by Waksman[16] and the International Streptomyces Project (ISP)[17] were used for studies of the morphological and cultural characterization, carbohydrate utilization and other taxonomic identification. The procedures of Hasegawa *et al.*[18] were used for chromatographic detection of the isomers of diaminopimelic acid and of major whole-cell sugars. 16S ribosomal DNA was amplified by PCR and the amplified fragment was sequenced directly. This strain was deposited in the National Institute of Advanced Industrial Science and Technology as FERM BP-8016.

^{1}H and ^{13}C NMR chemical shifts of A-503451 B (2) in $CDCl_3$

^{1}H NMR (500 MHz, $CDCl_3$, TMS)): δ 1.48 (1H, dt, J=4.4, 13.6 Hz), 1.57 (1H, dt, J=4.4, 13.6 Hz), 1.64 (3H, s), 1.64 (3H, s), 1.66 (3H, s), 2.01 (1H, dt, J=4.8, 12.5 Hz), 2.16 (1H, dt, 4.0, 12.5 Hz), 2.98 (1H, dd, J=9.2, 15.8 Hz), 3.08 (1H, dd, J=10.6, 15.8 Hz), 3.13 (3H, s), 3.44 (1H, d, J=9.2 Hz), 3.53 (1H, d, J=9.2 Hz), 4.17 (1H, dd, J=9.2, 9.9 Hz), 6.57 (1H, d, J=8.1 Hz), 7.77 (1H, d, J=1.5 Hz), 7.83 (1H, dd, J=1.8, 8.1 Hz). ^{13}C NMR (125 MHz, $CDCl_3$, TMS): δ 18.3, 20.0, 20.6, 28.1, 29.9, 32.6, 59.6, 66.3, 73.0, 78.5, 107.5, 118.7, 124.6, 126.6, 127.1, 128.1, 131.6, 155.9, 171.7.

2-(3,4-Dimethylpent-3-enyl)-2-(methoxymethyl)-3-[(methylsulfonyl) oxy]-1,2,3,4-tetrahydroquinoline-6-carboxylic acid (5)

To a solution of **4** (50 mg) in $CHCl_3$ (4 ml), triethylamine (560 µl) and methanesulfonylchloride (60 µl) were added under ice cooling and the mixture was stirred at room temperature for 2 h. The reaction was quenched by the addition of water. The pH of the mixture was adjusted to 4.5 and the resulting residue was extracted with ethyl acetate. The organic layer was concentrated to dryness to give an oily substance. The substance was purified by preparative HPLC using an ODS column (SYMMETRY C18, 19 i.d. x 100 mm, Waters Corp.) with MeCN-5 mM aq. NH_4OAc at pH 4.5 (2:1). The fraction containing **5** was concentrated and then **5** was extracted with ethyl acetate. The organic layer was washed with water and brine, dried over anhydrous Na_2SO_4 and concentrated to dryness to give **5** as a white powder (8.2 mg). APCI-MS (*m/z*): 412 $(M+H)^+$, 316 $(M-CH_3SO_3H+H)^+$. ^{1}H NMR (500 MHz, $CDCl_3$, TMS): δ 1.56 (1H, a (not clearly observed due to overlapping)), 1.58 (3H, s), 1.60 (3H, s), 1.60 (3H, s), 1.71 (1H, ddd, J=5.1, 12.1, 13.6 Hz), 2.04 (2H, m), 3.01 (3H, s), 3.15 (1H, dd, J=4.0, 18.0 Hz), 3.22 (1H, dd, J=3.7, 18.0 Hz), 3.43 (3H, s), 3.46 (1H, d, J=8.8 Hz), 3.59 (1H, d, J=8.8 Hz), 4.66 (1H, br. s), 5.07 (1H, t, J=3.5 Hz), 6.52 (1H, d, J=8.8 Hz), 7.77 (1H, d, J=9.0 Hz), 7.78 (1H, s). ^{13}C NMR (125 MHz, $CDCl_3$, TMS): δ 18.4, 19.9, 20.6, 27.7, 30.0, 33.3, 39.1, 57.2, 59.3, 72.7, 74.5, 113.5, 114.7, 117.7, 125.0, 126.2, 130.5, 132.6, 146.8, 171.3.

3-(Acetyloxy)-2-(3,4-dimethylpent-3-enyl)-2-(methoxymethyl)-1,2,3,4-tetrahydroquinoline-6-carboxylic acid (6)

To a solution of **4** (78 mg) in pyridine (5 ml), acetic anhydride (1.5 ml) was added at room temperature, and the resulting mixture was stirred for 14 h. The solvent was removed under reduced pressure, and the resulting residue was extracted with ethyl acetate. The organic layer was concentrated to dryness to give an oily substance. The substance was purified by preparative HPLC using an ODS column (SYMMETRY C18, 19 i.d. x 100 mm) with MeCN-0.3% TEAP buffer at pH 5.0 (3:2). The fraction containing **6** was concentrated and then **6** was extracted with ethyl acetate. The organic layer was washed with water and brine, dried over anhydrous Na_2SO_4, and concentrated to dryness to give **6** as a white powder (67.5 mg). ESI-MS (*m/z*): 414 $(M+K)^+$, 398 $(M+Na)^+$, 376 $(M+H)^+$, 316 $(M-CH_3COOH+H)^+$. ^{1}H NMR (500 MHz, $CDCl_3$, TMS): δ 1.59 (3H, s), 1.60 (3H, s), 1.60 (3H, s), 1.60 (1H, m), 1.73 (1H, m), 2.04 (3H, s), 2.04 (2H, m), 2.86 (1H, dd, J=4.4, 17.2 Hz), 3.13 (1H, dd, J=4.0, 17.2 Hz), 3.39 (3H, s), 3.39 (1H, d, J=8.5 Hz), 3.49 (1H, d, J=8.8 Hz), 4.75 (1H, br. s), 5.24 (1H, t, J=4.4 Hz), 6.52 (1H, d, J=8.4 Hz), 7.74 (1H, s), 7.76 (1H, dd, J=2.2, 8.4 Hz). ^{13}C NMR (125 MHz, $CDCl_3$, TMS): δ 18.4, 19.9, 20.6, 21.2, 28.0, 29.1, 33.4, 56.9, 59.4, 67.6, 73.3, 113.3, 115.9, 117.2, 124.6, 126.6, 130.2, 132.6, 147.4, 170.5, 171.5.

Detection of HIF activation

pGVB2-EPO luciferase reporter plasmid was constructed by inserting the 126-bp 3′ EPO (erythropoietin) enhancer (corresponds to nucleotide 120–245 on the 3′ side of the poly (A) addition site) and the 144-bp minimal EPO promoter (corresponds to nucleotide -118 to +26 relative to the transcription initiation site) into the upstream of the firefly luciferase of pGVB2 (Wako Pure Chemical Industries, Ltd., Osaka, Japan).

HepG2 cells were transfected with pGVB2-EPO and seeded at 5.0×10^3 cells per well in 96-well plates. After overnight incubation, test compounds were added to the plate. After 16 h of incubation, luciferase activity was determined with the use of Steady Glo Luciferase Assay System (Promega Corp., Fitchburg, WI, USA) following the manufacturer's instruction. Details of this assay were reported in a subsequent paper.

CONFLICT OF INTEREST

The authors declare no conflict of interest.

ACKNOWLEDGEMENTS

We are deeply grateful to Ms Yasuko Kono for assistance, and Dr Toshio Takatsu and Dr Masatoshi Inukai for their useful advice.

1 Park, J. W., Chun, Y. S. & Kim, M. S. Hypoxia-inducible factor 1-related diseases and prospective therapeutic tools. *J. Pharmacol. Sci.* **94**, 221–232 (2004).
2 Wang, G. L. & Semenza, G. L. Desferrioxamine induces erythropoietin gene expression and hypoxia-inducible factor 1 DNA-binding activity: implications for models of hypoxia signal transduction. *Blood* **82**, 3610–3615 (1993).
3 Liu, Y., Cox, S. R., Morita, T. & Kourembanas, S. Hypoxia regulates vascular endothelial growth factor gene expression in endothelial cells. Identification of 5' enhancer. *Circ. Res.* **77**, 638–643 (1995).
4 Zaman, K. *et al.* Protection from oxidative stress-induced apoptosis in cortical neuronal cultures by iron chelators is associated with enhanced DNA binding of hypoxia-inducible factor-1 and ATF-1/CREB and increased expression of glycolytic enzymes, p21(waf1/cip1), and erythropoietin. *J. Neurosci.* **19**, 9821–9830 (1999).
5 Zhao, S. & Wu, J. Hypoxia inducible factor stabilization as a novel strategy to treat anemia. *Curr. Med. Chem.* **20**, 2697–2711 (2013).
6 Nakagawa, A. *et al.* Virantmycin, a new antiviral antibiotic produced by a strain of *Streptomyces*. *J. Antibiot.* **34**, 1408–1415 (1981).
7 Kobayashi, H., Ohyama, T., Kitamura-Miyazaki, M., Hirota-Takahata, Y. & Ando, O. Studies on novel HIF activators, A-503451s II. Biological activities of A-503451 A. *J. Antibiot.* **69**, 754–758 (2016).
8 Kim, O. S. *et al.* Introducing EzTaxon-e: a prokaryotic 16S rRNA gene sequence database with phylotypes that represent uncultured species. *Int. J. Syst. Evol. Microbiol.* **62**, 716–721 (2012).
9 Morimoto, Y. & Shirahama, H. Synthetic studies on virantmycin. 2. Total synthesis of unnatural (+)-virantmycin and determination of its absolute stereochemistry. *Tetrahedron* **52**, 10631–10652 (1996).
10 Meissner, A. & Sørensen, O. W. Measurement of *J*(H,H) and long-range *J*(X,H) coupling constants in small molecules. Broadband XLOC and J-HMBC. *Magn. Reson. Chem.* **39**, 49–52 (2001).
11 Matsumori, N., Kaneno, D., Murata, M., Nakamura, H. & Tachibana, K. Stereochemical determination of acyclic structures based on carbon-proton spin-coupling constants. A method of configuration analysis for natural products. *J. Org. Chem.* **64**, 866–876 (1999).
12 Kim, W.-G., Kim, J.-P., Koshino, H., Shin-Ya, K., Seto, H. & Yoo, I.-D. Benzastatins E, F and G: New indoline alkaloids with neuronal cell protecting activity from *Streptomyces nitrosporeus*. *Tetrahedron* **53**, 4309–4316 (1997).
13 Pearce, C. M. & Sanders, J. K. Stereochemistry of (-)-virantmycin. *J Chem Soc Perkin Trans.* **1**, 409–411 (1990).

14 Kim, W.-G., Kim, J.-P., Kim, C.-J., Lee, K.-H. & Yoo, I.-D. Benzastatins A, B, C and D : new free radical scavengers from *Streptomyces nitrosporeus* 30643 I. Taxonomy, fermentation, isolation, physico-chemical properties and biological activities. *J. Antibiot.* **49**, 20–25 (1996).
15 Kim, W.-G., Kim, J.-P. & Yoo, I.-D. Benzastatins A, B, C and D : new free radical scavengers from *Streptomyces nitrosporeus* 30643 II. Structure determination. *J. Antibiot.* **49**, 26–30 (1996).
16 Waksman, S. A. in *The Actinomycetes Classification, Identification and Description of Genera and Species* Vol. 2 (ed. Waksman S. A.) (The Williams & Wilkins Company press, USA, 1961)
17 Shirling, E. B. & Gottlieb, D. Methods for characterization of *Streptomyces* species. *Int. J. Syst. Bacteriol.* **16**, 313–340 (1966).
18 Hasegawa, T., Takizawa, M. & Tanida, S. A rapid analysis for chemical grouping of aerobic actinomycetes. *J. Gen. Appl. Microbiol* **29**, 319–322 (1983).